

Research Article

Movie Special Effects Processing Based on Computer Imaging Technology

Yidong Cheng  and **Yi Wang**

Sejong University, Seoul 05006, Republic of Korea

Correspondence should be addressed to Yidong Cheng; 16115291@bjtu.edu.cn

Received 23 November 2021; Revised 9 December 2021; Accepted 16 December 2021; Published 10 January 2022

Academic Editor: Le Sun

Copyright © 2022 Yidong Cheng and Yi Wang. This is an open access article distributed under the Creative Commons Attribution License, which permits unrestricted use, distribution, and reproduction in any medium, provided the original work is properly cited.

The film space is the image of social life represented on the screen, which determines that the form of the film and television picture is a plane model, and it can only use a two-dimensional plane space to express an objective scene with a three-dimensional space. In order to improve the effects of special effects processing in movies, this paper applies computer imaging technology to the processing of movie characteristics. When performing specific scene simulations, the specific structure of each computer imaging particle system is derived on the basis of the general structure of the computer imaging particle system. In addition, this paper combines the improved algorithm to carry out several case analyses, and the reliability of this method is verified through simulation experiments, which promotes the application and promotion of computer imaging technology in movie special effects processing.

1. Introduction

With the development of the economy and the advancement of science and technology, computers have gradually become small and compact from giants. Gradually, ordinary people can also purchase computers, which were very high-tech machines in the past. The gradual popularization of computers has quietly changed the development direction of all walks of life. The film special effects modeling industry eager for new technologies quickly absorbed the fresh blood of computer technology and began to develop in a new direction, and film special effects came into being [1]. Before being impacted by digital special effects, physical special effects prevailed, and all the characters imagined by people need to be realized by the technical means of physical sculpture. However, after the prevalence of computer technology, special effects technology gradually made special effects modeling virtual, and special effects scenes and characters completed the transition from realization to virtualization. This has a certain inevitability. Before computer technology took shape, the physical special effects of entities had been very strenuous in order to satisfy people's

powerful imagination, and the physical special effects could no longer satisfy people's increasingly romantic and exaggerated imagination of movies. Moreover, excellent physical effects studios such as Winston Studio seem to have achieved the ultimate in physical effects, so it is difficult to have new possibilities [2]. At this time, the emergence of computer special effects is just right for the film special effects industry.

Movie is a kind of audiovisual art expressed through pictures, and pictures are the basic elements of movies. The sense of space of the screen is particularly important in the modeling of the film and television screen and the three-dimensional space of the screen scene [3].

The reason why film and television can become an art is that it can use various methods and means to overcome its own shortcomings and show itself more perfectly. People have determined the direction of space according to the direction of the sun, and the east, south, west, north, southeast, northeast, southwest, and northwest are collectively referred to as all directions. We call the depth of space. In reality, the space we are in is a three-dimensional space. Objects can be stationary in a fixed position in space, or they can change their own position by moving in any direction in

all directions of spatial location. This kind of spatial position movement will cause changes in the spatial distance when moving away from the viewpoint or approaching the viewpoint. The spatial form refers to the length, width, and height of the space occupied by an object when it is in a three-dimensional space. When the specific values of these three dimensions are determined, then the specific spatial form of the object is also determined. In reality, people's perception of external objects is specific and tangible. In the absence of specific and accurate three-dimensional values, one can still determine its spatial form by perceiving the three-dimensional proportions of external objects based on existing experience.

The form of an object in space can be divided into two- and three-dimensional spatial forms. Two-dimensional space is usually a flat surface, and the displayed objects have only length and width. From this point of view, the film screen is a two-dimensional spatial form, which belongs to graphic art. The real objective world is a three-dimensional space. The objects in this world represent the three-dimensional space form. The biggest difference from the two-dimensional plane form is that the three-dimensional space form has spatial depth. Therefore, graphic arts such as paintings and photographs are suitable for expressing things in two-dimensional space, and objects with spatial depth need to be expressed in a three-dimensional space. What film art needs to do is to accommodate objects in three-dimensional spatial form on a limited two-dimensional space plane and to express the three-dimensional visual characteristics of the object to be photographed on the two-dimensional plane.

This paper applies computer imaging technology to the process of film characteristics processing and studies the essence of film special effects processing, which provides a theoretical reference for the further development of subsequent film special effects processing technology.

2. Related Work

Three-dimensional technology is a product of the combination of graphic calculus and art school rapid expression [4]. It is more expressive and more attractive than traditional two-dimensional animation art. With the rapid development of science and technology, the tastes of the audience continue to improve. This method is obviously more in line with the aesthetic characteristics and advantages of modern people [5]. Therefore, it has to be admitted that Disney's 3D animation films have more vitality and market appeal than traditional 2D animations. The development of animation film special effects and the development of computers are inseparable. The traditional two-dimensional animation is to first draw the characters in action on paper according to the action scene cartoon animator and then copy them to the top of the cartoon characters [6].

The development of plane technology and the formation of application software in the computer three-dimensional effect, so far, have gone through several decades. With the rapid development of computer hardware and computer-intensive computer graphics technology, computer-

generated false scenes and special effects are no longer a fantasy [7]. The subtle performance of animation technology perfectly expresses the artistic beauty, art, and technology as a solid foundation; technology and art are constantly sublimated. The computer can generate a virtual world that is enough to be fake [8]. This depends on the modeling, rendering, and animation technology related to computer animation expertise and motion control synthesis technology [9]. Although many software has advanced to other technical levels, higher requirements have been put forward for the flexibility and controllability of the scene movement. The LED is more of an animation design-type technology; at the same time, due to its simplicity and compatibility, there is a widespread concern in the polygonal mesh model of the computer animation system [10].

Literature [11] studied the real-time lighting rendering of nonuniform participating media and proposed a real-time lighting rendering method for participating media in a virtual indoor environment. In terms of the specific implementation, by using 3D textures to organize nonuniform participating media, real-time rendering is realized: combining shadow mapping, volume shadowing, and light stepping technologies; a method of object volume shadowing considering the role of participating media is described hybrid drawing methods. Literature [12] studied the rendering of scattering materials and proposed an efficient algorithm based on Woodcock tracking. First, the traditional light stepping (ray marching algorithm) was implemented, and multiple comparison experiments were performed to verify the implementation, including the comparison of homogeneous participating media (homogeneous) and nonuniform participating media (heterogeneous), single scattering, and multiple subscattering. Then a more efficient Woodcock tracking algorithm is implemented, and the rendering efficiency and rendering effect of the two algorithms are compared. Literature [13] proposed a variant algorithm. It can use any selected cross-section. It is not the main cross-section of the entire system to sample the free flight distance. This technique avoids the main shortcomings of traditional Woodcock sampling and shows the theoretical derivation of heterogeneous media. Literature [14] proposed a one-dimensional analysis and numerical model. It is used for the basic optimization study of free sampling parameters and demonstrates the application case description using GPU-based Monte Carlo code for radiotherapy.

In computer graphics, participatory media is usually described as a collection of scattering microscopic particles (although described as particles, fluid media is also applicable to these theories. For the convenience of introduction, the explanation of the theory will be continued later. Following the term "particles"), due to the small size of these particles and the characteristics of random distribution, we generally do not describe the interaction of individual particles but consider the probabilistic behavior of the entire collection of particles [15]. When a photon passes through a medium composed of a group of microscopic particles, it may not collide with any particles at all and continue to travel freely (just like in a vacuum), or it may interact with

some of the particles, thereby affecting the transmission of light [16]. The probability of interaction between photons and particles depends on the extinction coefficient of the medium, also known as the attenuation coefficient, which is represented by a variable named σ . The size of the extinction coefficient depends on the density of the medium and other physical characteristics. It is the result of the interaction of two types of illumination: when a photon interacts with a particle, the photon is either absorbed by the particle or scattered to another direction [17].

3. Computer Molding Technology

At present, it is an era of digital information processing. Under the condition of limited bandwidth resources, people have higher and higher requirements for signal sampling rate and processing speed. Information processing in the traditional sense is to compress after a large amount of sampling, thereby reducing the pressure of signal transmission and storage. This method often causes a large amount of waste of sampling information.

We assume that the discrete signal in an n -dimensional domain space is $x \in R^n$ and an orthonormal basis in the space is $\psi \in R^{m \times n}$, and the signal x can be uniquely linearly represented by the basis matrix ψ as follows [18]:

$$x = \psi\alpha, \quad (1)$$

where α is the linear representation coefficient of the signal x on the base matrix A . If there are many items that are equal to or have values close to zero in the representation coefficients obtained by using the above transformation on the signal, then it can be said that the signal has sparseness under the base matrix. In particular, when the number of nonzero elements in the coefficient vector α is k , the signal x is called a sparse signal representing k on the basis matrix ψ .

The above x and α can be regarded as representations of the same signal in different domains, and there may be cases where the signal x is not compressible in the domain space α but is compressible in the domain space ψ . This characteristic of the signal is used in many applications, such as wavelet transform in image processing. The value of each pixel in the original image is almost nonzero in the spatial domain, but it is very sparse in the wavelet domain representation, and there are only a few nonzero coefficients. In the image restoration process, only the limited nonzero coefficients are needed to approximate the original image well. However, in traditional signal processing, transform coding only exists in the signal compression process, and a large amount of sampling information is still needed in the sampling stage, which causes a serious waste of sampling information.

Compressed sensing theory proposes to compress the sparse signal x in formula (1), that is, it uses a random measurement matrix $\Phi \in R^{m \times n}$ that is not correlated with the base matrix ψ or has little correlation to sample x . In the process of sampling, data compression is completed, and the number of sampling is $m_c \geq k \log(n/k)$ ($m_c \ll n$), thus greatly

reducing the waste of sampling information. The sampling result is expressed as follows [19]:

$$y = \Phi x, \quad (2)$$

where $y \in R^m$ is called the observed value, which is not the signal itself but the projection value of the signal from high to low dimensions. When the sparse representation of x is incorporated into the above formula, we can get:

$$y = \Phi x = \Phi \psi \alpha. \quad (3)$$

Finally, the original signal x can be recovered approximately by reconstructing the observed value y . The specific method is in the known base matrix ψ , by solving the optimization problem [20]:

$$\begin{aligned} & \underset{\{\alpha\}}{\text{minimize}} \|\hat{\alpha}\|_0 \\ & \text{subject to } \|y - \Phi \psi \hat{\alpha}\|_2 \leq \varepsilon. \end{aligned} \quad (4)$$

We get a $\hat{\alpha}$ with the smallest number of nonzero values and recover the original signal $x \approx \hat{x} = \psi \hat{\alpha}$, where ε is the threshold of the fitting error.

The sparse characteristic of the signal itself or the sparse representation in a certain transform domain is the basis for the application of compressed sensing. For the definition of signal sparsity, when the number of nonzero elements in the coefficient vector of the signal in the base matrix is k , the signal is called a k -sparse signal. When the coefficient vector of the signal under the base matrix satisfies the equation [21]:

$$\|\alpha\|_p = \left(\sum_i |\alpha_i|^p \right)^{1/p} \leq R. \quad (5)$$

The signal is sparse, and the range of p and R in the formula is $0 < p < 2$ and $R > 0$. In general, the degree of sparse representation of the signal under different base matrices ψ is not the same. Therefore, in practical engineering applications, the most appropriate sparse representation base needs to be selected. Usually, in signal processing, a large number of transform bases are used in the frequency domain, such as Fourier transform bases, discrete cosine transform bases, and wavelet transform bases. By using them, the original signal can be projected into the corresponding new space, and the processing that the signal cannot achieve in the original domain, such as spectrum analysis and frequency domain filtering, can be completed. In addition, the commonly used basis matrices include curvelet basis, Gabor basis, and so on.

The representation of the measurement matrix is $\Phi \in R^{m \times n}$, and $m \ll n$. The effect of the above measurement matrix can be expressed mathematically as follows:

$$y = \Phi x = \Phi \psi \alpha \text{ or } y = \Phi \alpha = \Phi \psi^T x. \quad (6)$$

That is, the signal or the sparse representation coefficient vector of the signal is projected to obtain the measured value $y \in R^m$. The ultimate goal of compressed sensing is to recover the signal x or its sparse representation coefficient vector α through the measured value y . In fact, it is to solve

equation (6). This process is a mapping process from a low-dimensional signal (m -dimensional) to a high-dimensional signal (n -dimensional), which solves an underdetermined system of equations. In theory, this underdetermined problem has an infinite number of solutions, but the signal processed by compressed sensing is sparse. The signal x is a k -sparse signal ($k \ll m$), so formula (6) is solvable under this premise.

For any signal x with a sparsity of k , if the equation is satisfied:

$$(1 - \delta_k) \|k\|_{l_2}^2 \leq \|\tilde{\Phi}\xi\|_{l_2}^2 \leq (1 + \delta_k) \|x\|_{l_2}^2, \delta_k \in [0, 1], \quad (7)$$

where $\tilde{\Phi} = \Omega\psi$ (or $\Phi\psi^T$) is the compressed sensing matrix; then $\tilde{\Phi}$ at this time satisfies the constraint equidistance condition. In practical applications, it is very difficult to select the measurement matrix through the principle of formula (7), and solving it is a problem of combinatorial complexity. When the measurement matrix Φ is not related to the base matrix ψ , the compressed sensing matrix $\tilde{\Phi}$ satisfies the constraint equidistance condition with a high probability. The uncorrelation at this time means that the measurement matrix and the base matrix cannot be sparsely represented by each other. When the irrelevance is stronger, the more the information of the signal x carried in the measurement value y , the higher the success rate of signal reconstruction.

Therefore, when designing the measurement matrix, it is necessary to consider the constraint equidistance condition or the principle of noncorrelation. At present, the commonly used measurement matrices are random matrices, such as random Gaussian matrix, random Bernoulli matrix, random Toeplitz matrix, and so on.

The third key part of compressed sensing is the signal reconstruction algorithm. A good reconstruction algorithm will improve the efficiency and accuracy of signal reconstruction.

The signal reconstruction algorithm needs to solve the problem of recovering the signal x from the measurement result y described in equation (3) or (6). The signal optimization problem described by equation (4) can be expressed as a Lagrangian equation. In the solution process, the signal reconstruction error and the coefficient sparsity level are weighed into consideration, expressed as follows:

$$\underset{\{\alpha\}}{\text{minimize}} \|y - \Phi\psi\hat{\alpha}\|_2 + \lambda \|\hat{\alpha}\|_0. \quad (8)$$

Equations (4) and (8) are essentially underdetermined equations. The ℓ_0 -norm problem in the equation is a non-deterministic polynomial hard (NP-hard) problem. Two types of methods commonly used to solve such problems are greedy methods and convex relaxation methods.

The greedy method has low computational complexity and fast execution speed in sparse signal reconstruction, but its accuracy is relatively low. Contrary to the convex relaxation method, the accuracy of signal approximation is greatly improved. The core idea of this kind of method is to replace the ℓ_0 -norm that causes NP-hardness in the original problem with the convex ℓ_1 -norm so as to transform the NP-

hard problem into a related convex problem. Studies have proved that this kind of replacement is possible with a high probability.

When the basis pursuit (BP) in the convex relaxation method solves the convex problem, the ℓ_0 norm in (4) is replaced with the ℓ_1 norm, and the measured value y is constrained by the equation, expressed as follows:

$$\underset{\{\alpha\}}{\text{minimize}} \|\hat{\alpha}\|_0 \text{ subject to } y = \Phi\psi\hat{\alpha}. \quad (9)$$

When the number of samples meets $m_c \geq k \log(n/k)$, base tracking can get good results. The basis tracking denoising (BP denoising; BPDN), which is similar to basis tracking, can well suppress the noise signal in the process of solving. The problem it deals with can be expressed as follows:

$$\underset{\{\alpha\}}{\text{minimize}} \|\hat{\alpha}\|_0 \text{ subject to } \|y - \Phi\psi\hat{\alpha}\|_2 \leq \varepsilon. \quad (10)$$

Unlike equation (9), it uses an inequality to constrain the measured value y . These two methods for solving convex problems can be summarized as: minimizing the sparsity of coefficient vectors while satisfying the approximation error. In addition, methods for solving convex problems include the lasso algorithm (Lasso), the interior point method, and so on.

The convex relaxation method can obtain the global optimal approximation result, and the solution accuracy is high, but the calculation time is longer than that of the greedy method. Therefore, in practical applications, we can choose a suitable signal reconstruction algorithm according to specific requirements.

The object displayed in the light-field three-dimensional display can be regarded as composed of many three-dimensional points, and the light field can be expressed as a five-dimensional plenoptic function: $L = L_{O_1}(x_i, y_i, z_i, \theta, \phi)$. This chapter uses the two-plane parameterization method to parameterize the light field in the analysis process of calculating the light field collection. The specific description is: in the free space without occlusion, the intensity of light will not attenuate during the propagation process. The five-dimensional plenoptic function L can be reduced to four-dimensional and mathematically described as the flow of light energy along the light in the three-dimensional space. It is produced by the diffuse reflection, specular reflection, and ambient light from the surface of the object to the light emitted by the light source. For visualization purposes, light rays can be described as a line connecting them with the intersection of two parallel planes separated by a unit distance, that is, the line connecting the first plane point pair $u = \{u_i, v_i\}$ and the second plane point pair $s = \{s_i, t_i\}$ shown in Figure 1. The light field at this time is the collection of all rays in the scene, which can be expressed as $I\{u_i, v_i, s_i, t_i\}$, which is a four-dimensional representation. In the rest of this chapter, the light field is abbreviated as $l(u, s)$.

In the two-plane parameterization method of the light field, a plane can be placed at infinity, and the light at this time can be parameterized as a point plus a direction. This kind of parameterization is very useful for constructing the

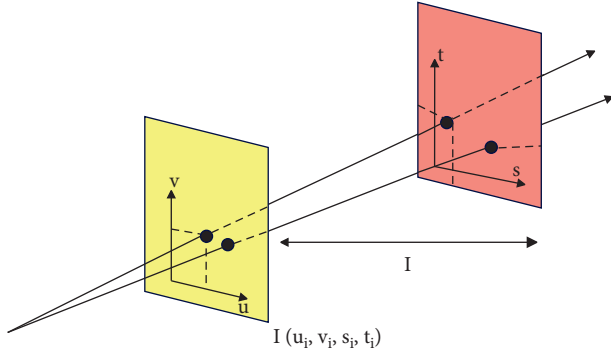


FIGURE 1: Two-plane parameterization of the four-dimensional light field.

light field because the light field at this time can be regarded as a set of images within a certain angle of view. In addition, the geometric operation efficiency of this parameterization method is very high. The specific performance is that the process of light mapping to plane points and the process of inverse mapping of image pixels to light are linear problems, which can be realized by multiplying by a matrix.

$$\begin{aligned}
 L_0(f_u, f_s) &= \int_{u'=-\infty}^{\infty} \int_{s=-\infty}^{\infty} l_0(u', s) e^{-2i\pi f_u(u'+2s)} e^{-2i\pi f_s s} du' ds \\
 &= \int_{u'=-\infty}^{\infty} \int_{s=-\infty}^{\infty} l_0(u', s) e^{-2i\pi f_u u'} e^{-2i\pi(f_s + z f_u)s} du' ds \\
 &L(f_u, f_s + z f_u),
 \end{aligned} \tag{13}$$

where $L_0(f_u, f_s)$ and $L(f_u, f_s)$ represent the Fourier transform corresponding to $l_0(u, s)$ and $l(u, s)$, respectively. It can be clearly seen from $L_0(f_u, f_s)$ that the spectrum after propagation has undergone shear along the f_s dimension, and the longer the propagation distance, the more obvious the shear.

When the light is occluded, its intensity value is equivalent to multiplying by an occlusion function and becomes:

$$l_0(u, s) = l(u, s)O(u, s). \tag{14}$$

When it is completely occluded, the occlusion function $O(u, s) = 0$; $O(u, s) = 1$ is the case of no occlusion. When $0 < O(u, s) < 1$, it is occluded to varying degrees. The position where the light is blocked depends entirely on the spatial dimension u . The Fourier transform form of the occlusion process is as follows:

$$L_0(f_u, f_s) = L(f_u, f_s) * O(f_u, f_s). \tag{15}$$

In general, the occluder will affect the spatial dimension u and the angular dimension s of the light at the same time, and the influence on the angular dimension is related to the depth range of the occluder. In particular, when the occluder is a plane occluder and is perpendicular to the light, its

We analyze in advance the phenomena that occur during the propagation of the light field and the corresponding changes in the light field after the phenomena occur. For the two-plane parameterized light field $l(u, s)$, its Fourier transform is expressed as follows:

$$L = (f_u, f_s) = \int_{u=-\infty}^{\infty} \int_{s=-\infty}^{\infty} l(u, s) e^{-2i\pi f_u u} e^{-2i\pi f_s s} du ds. \tag{11}$$

When the light field propagates in free space, the intensity of the light will not change, but its angular dimension (direction dimension) and spatial dimension will change. Therefore, the process of light field propagation is actually the reparameterization of the light field. If it is assumed that z is the distance traveled by the light field $l(u, s)$, the light field at this time can be expressed as follows:

$$l_0(u, s) = l(u - zs, s). \tag{12}$$

The corresponding Fourier transform is as follows:

occlusion function is a constant in the angular dimension s , and the corresponding Fourier transform is a unit pulse.

4. Movie Special Effects Processing Based on Computer Imaging Technology

When simulating a specific scene, we derive the specific structure of each computer imaging particle system on the basis of the general structure of the computer imaging particle system. The general structure of the computer imaging particle system is shown in Figure 2. The computer imaging particle system is generally composed of computer imaging particle management, computer imaging particle storage, and computer imaging particle rendering.

In the computer imaging particle system, each computer imaging particle must undergo three life courses: birth, dynamic change, and extinction. The algorithm framework of the computer imaging particle system is shown in Figure 3.

In order to simplify the calculation, the distribution area can be replaced by a rectangular parallelepiped in front of the viewpoint without affecting the realism of the graphics. The normal vector of a certain surface of the rectangular parallelepiped passes through the viewpoint, and the initial distribution area of the computer imaging particles is a

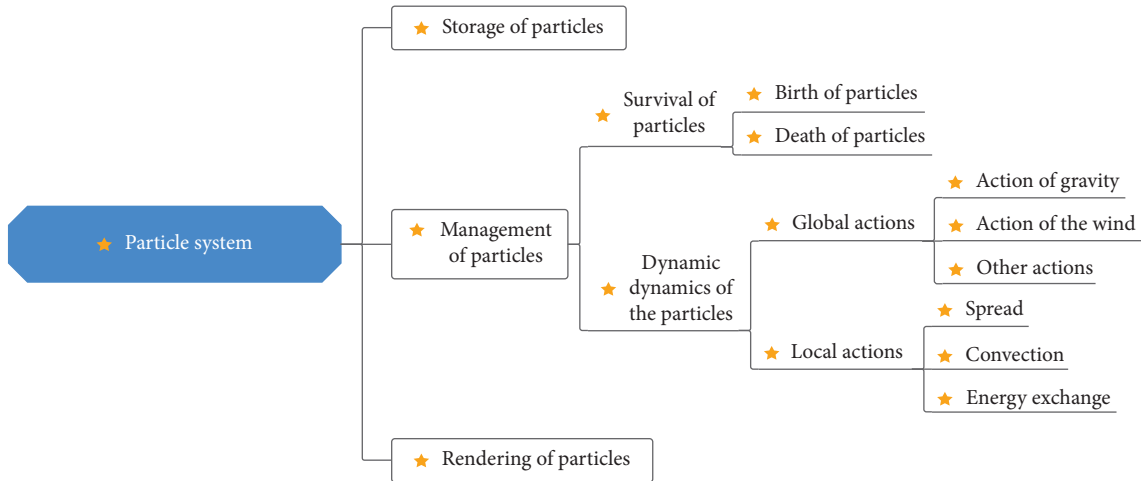


FIGURE 2: General structure of computer imaging particle system.

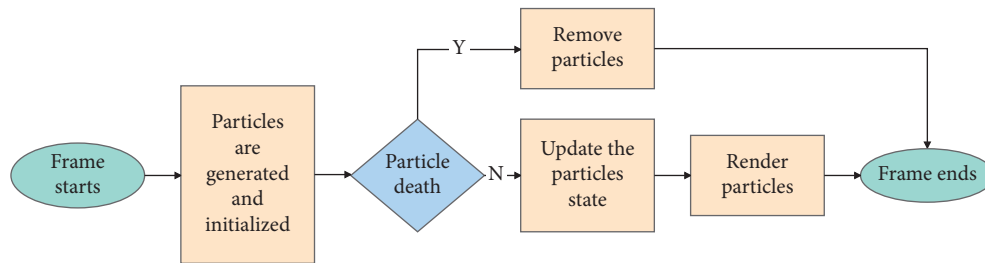


FIGURE 3: Algorithm framework of computer imaging particle system.

surface parallel to the XOZ surface in the rectangular parallelepiped, and its normal is facing downwards. The schematic diagram of the distribution area is shown in Figure 4.

When setting the spatial location properties of raindrops, the algorithm still takes the principle of not affecting the real effects of raindrops, and the main goal is to maximize the number of particles in computer imaging. Moreover, it also designs the spatial position distribution area of the raindrop computer imaging particles in a deep area within the viewing cone. However, because the raindrop itself is greatly affected by gravity, the initial spatial position of the raindrop can be distributed on a quarter of a sphere with the viewpoint as the center of the sphere, including the viewing cone, as shown in Figure 5.

The fountains seen in real life consist of spraying hair out of the body of water, and under certain water pressure, a column of water is emitted upwards and then spreads around to form fountains of different shapes. The entire fountain body can be regarded as multiple parabolic water columns emitted from the surrounding by the central nozzle, and each water column is composed of multiple water columns, as shown in Figure 6. The fountain model is special. The special feature is that the computer imaging particles of water droplets in the fountain water are not independent individuals, but the computer imaging particles of water droplets have a certain adhesive force between them, which makes the computer imaging

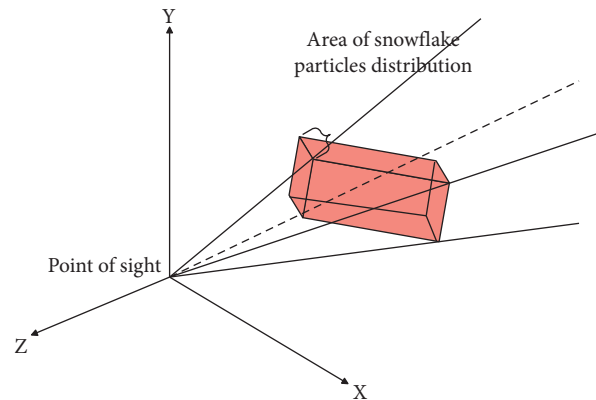


FIGURE 4: Schematic diagram of the computer imaging particle distribution area of snowflake.

particles of water droplets stick together to form larger water droplets.

The implementation modules of the system are divided into the following two categories in terms of function. The first is the basic function module, which is composed of two modules, a memory management module and a mathematical basic module, mainly to provide memory and data operation support for the system. The other is the system core module, which consists of four modules: system control module, scene management module, computer imaging particle system management module, and graphics

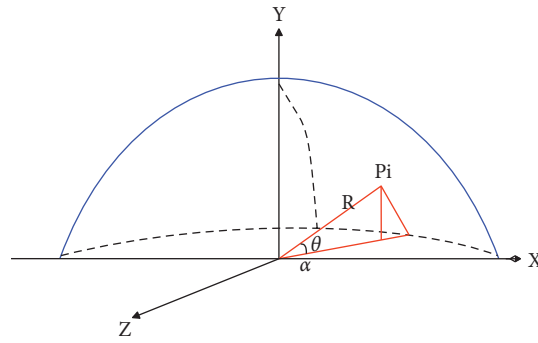


FIGURE 5: Schematic diagram of the computer imaging particle distribution area of raindrops.

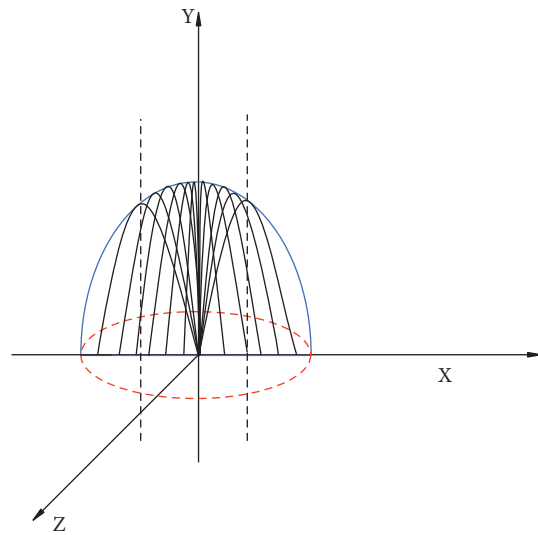


FIGURE 6: Fountain model diagram.

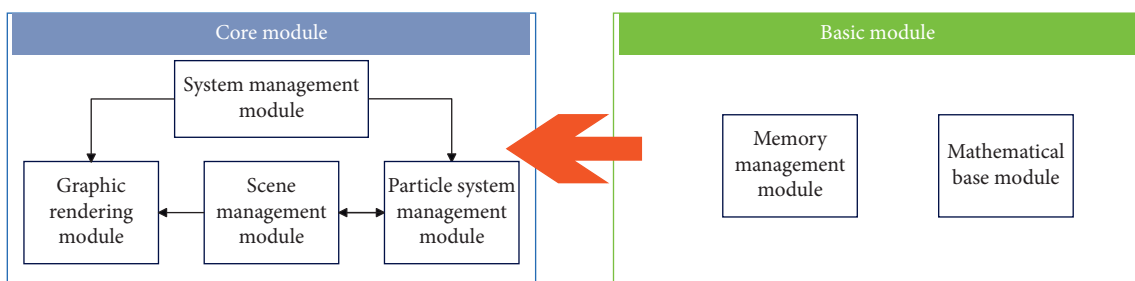


FIGURE 7: Macroscopic architecture diagram of 3D computer imaging particle special effects system.

rendering module. The system architecture of the 3D computer imaging particle special effects system is shown in Figure 7.

On this basis, we need to clarify the processing flow of the system. Figure 8 shows the brief processing flow of the system.

In order to better simulate various irregular sceneries with complex shapes and strengthen the management of natural sceneries, object-oriented thinking is adopted, and the concept of the hierarchical structure of computer

imaging particle systems is introduced. The hierarchical structure of the computer imaging particle system is shown in Figure 9:

The processing flow of the control submodule is shown in Figure 10:

After constructing the system, the system is simulated and studied; TV special effects processing is simulated; and the computer imaging effects and film special effects processing effects of the system in this paper are evaluated, and the results are shown in Table 1 and Figure 11 are obtained.

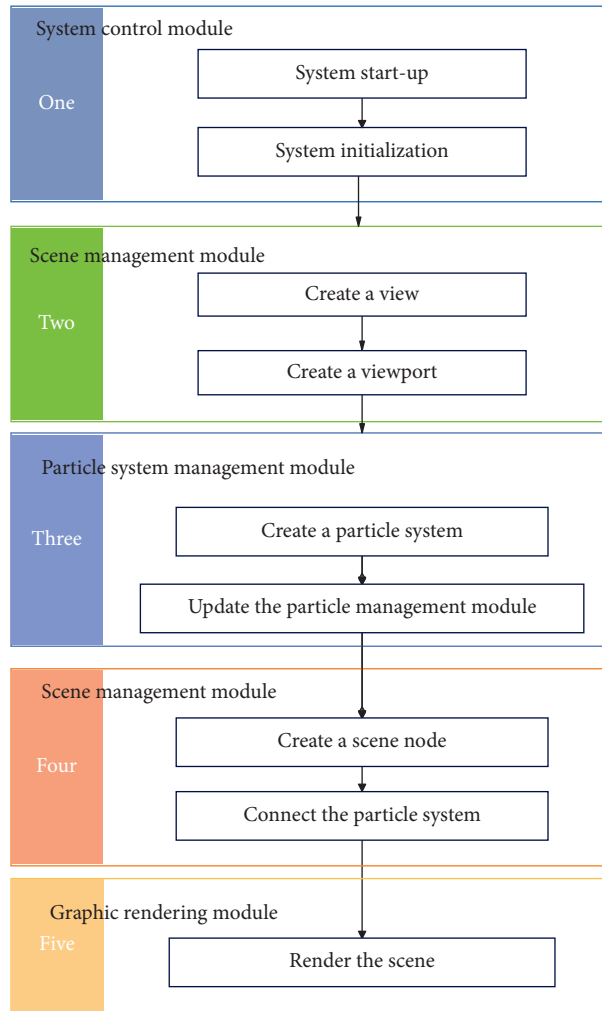


FIGURE 8: Process flow chart of computer imaging particle system.

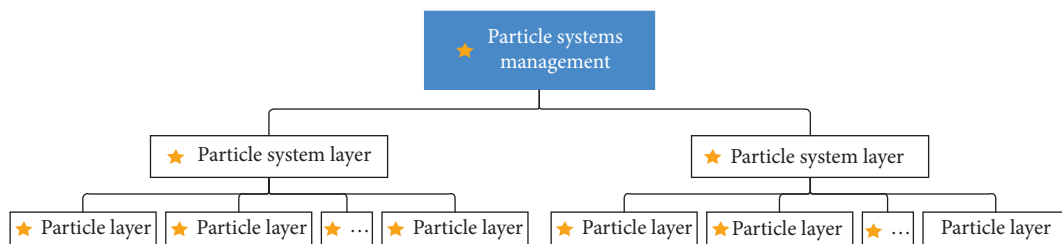


FIGURE 9: The hierarchical structure of computer imaging particle system.

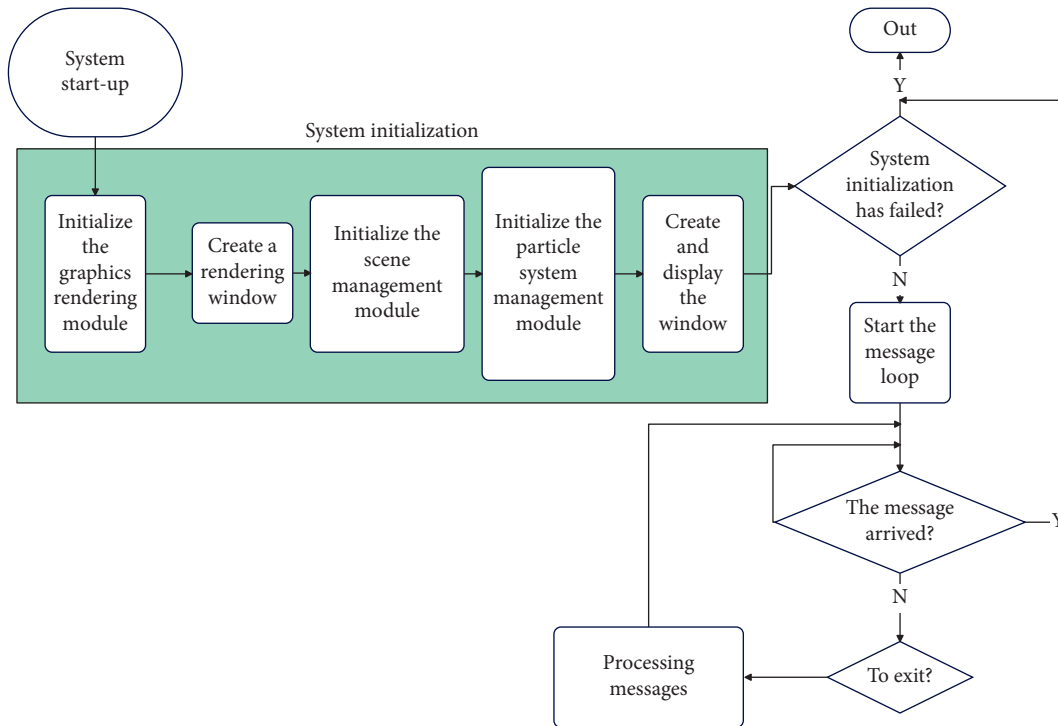


FIGURE 10: The execution flow chart of the control submodule.

TABLE 1: Evaluation of movie special effects processing effect based on computer imaging technology.

No.	Imaging effect	Special effects processing	No.	Imaging effect	Special effects processing
1	94.14	89.25	18	92.21	88.19
2	92.52	90.12	19	91.96	88.28
3	92.45	92.24	20	95.61	87.34
4	93.16	89.99	21	95.29	84.26
5	92.46	84.91	22	95.22	89.47
6	94.43	89.30	23	91.11	85.78
7	95.75	88.45	24	93.10	86.96
8	94.18	90.84	25	95.09	85.82
9	94.83	92.19	26	94.96	86.86
10	92.03	91.79	27	93.40	91.15
11	94.23	85.58	28	95.77	92.96
12	91.25	88.28	29	91.71	86.70
13	95.94	88.41	30	94.54	92.83
14	95.03	85.08	31	93.39	90.28
15	92.38	85.13	32	93.44	91.84
16	92.19	91.22	33	93.85	86.98
17	95.90	87.43	34	91.20	88.88

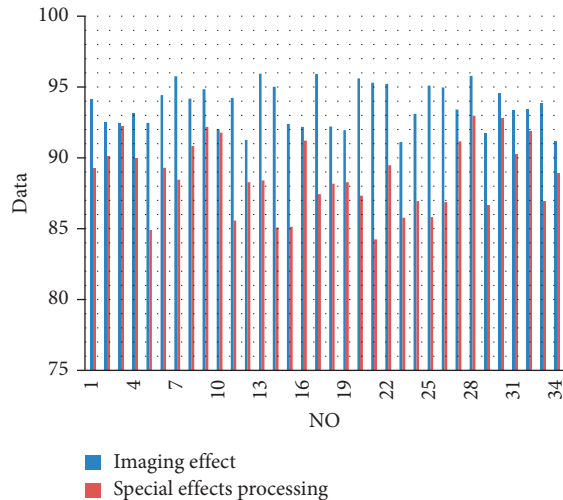


FIGURE 11: Statistical diagram of system performance.

Through the above experimental research, it can be seen that the film special effects processing method based on computer imaging technology proposed in this paper has good practical effects, and the computer imaging effects and film special effects processing effects are very good.

5. Conclusion

The construction of the film and television picture is in the same vein as the composition of the painting, so naturally, it is necessary to pay attention to the sense of space in the picture. The sense of space of the movie screen is formed by the combination of the composition of the screen, the perspective relationship of objects, and the visual illusion of people. Filmmakers must focus on the cross-composition of two-dimensional screen planes and three-dimensional projection elevations to develop the thinking of film space through the selection of film specifications and picture formats, the skills of framing and composition, and the processing of in-depth scheduling so as to realize the space design of the film screen up, down, left, and right. The truth of the picture depends on the understanding of the picture space. This paper applies computer imaging technology to the process of film characteristics processing and studies the essence of film special effects processing. The experimental results show that the movie special effects processing method based on computer imaging technology proposed in this paper has good practical effects, and the computer imaging effects and movie special effects processing effects are very good.

Data Availability

The labeled data set used to support the findings of this study is available from the corresponding author upon request.

Conflicts of Interest

The authors declare that there are no conflicts of interest.

Acknowledgments

This study was sponsored by Sejong University.

References

- [1] L.-C. Cheng and C.-L. Huang, "Exploring contextual factors from consumer reviews affecting movie sales: an opinion mining approach," *Electronic Commerce Research*, vol. 20, no. 4, pp. 807–832, 2020.
- [2] I. Spielvogel, B. Naderer, and J. Matthes, "Again and again: exploring the influence of disclosure repetition on children's cognitive processing of product placement," *International Journal of Advertising*, vol. 39, no. 5, pp. 611–630, 2020.
- [3] J. Steffens, "The influence of film music on moral judgments of movie scenes and felt emotions," *Psychology of Music*, vol. 48, no. 1, pp. 3–17, 2020.
- [4] G. Schalk, C. Kapeller, C. Guger et al., "Facephenes and rainbows: causal evidence for functional and anatomical specificity of face and color processing in the human brain," *Proceedings of the National Academy of Sciences*, vol. 114, no. 46, pp. 12285–12290, 2017.
- [5] S. Han, B. Liu, R. Wang, Y. Ye, C. D. Twigg, and K. Kin, "Online optical marker-based hand tracking with deep labels," *ACM Transactions on Graphics*, vol. 37, no. 4, pp. 1–10, 2018.
- [6] D. Stawarczyk, M. A. Bezdek, and J. M. Zacks, "Event representations and predictive processing: the role of the midline default network core," *Topics in Cognitive Science*, vol. 13, no. 1, pp. 164–186, 2021.
- [7] A. G. Sares, N. E. V. Foster, K. Allen, and K. L. Hyde, "Pitch and time processing in speech and tones: the effects of musical training and attention," *Journal of Speech, Language, and Hearing Research*, vol. 61, no. 3, pp. 496–509, 2018.
- [8] A. K. Fishell, T. M. Burns-Yocum, K. M. Bergonzi, A. T. Eggebrecht, and J. P. Culver, "Mapping brain function during naturalistic viewing using high-density diffuse optical tomography," *Scientific Reports*, vol. 9, no. 1, pp. 11115–11211, 2019.
- [9] E. Peters and C. Muñoz, "Introduction to special issue Language learning from multimodal input," *Studies in Second Language Acquisition*, vol. 42, no. 3, pp. 489–497, 2020.
- [10] C. Li, Z. Wang, Y. Lu, X. Liu, and L. Wang, "Conformation-based signal transfer and processing at the single-molecule level," *Nature Nanotechnology*, vol. 12, no. 11, pp. 1071–1076, 2017.
- [11] N. Molinaro and M. Lizarazu, "Delta (but not theta)-band cortical entrainment involves speech-specific processing," *European Journal of Neuroscience*, vol. 48, no. 7, pp. 2642–2650, 2018.
- [12] Y. Deldjoo, M. F. Dacrema, M. G. Constantin et al., "Movie genome: alleviating new item cold start in movie recommendation," *User Modeling and User-Adapted Interaction*, vol. 29, no. 2, pp. 291–343, 2019.
- [13] R. Piryani, V. Gupta, and V. K. Singh, "Movie Prism: a novel system for aspect level sentiment profiling of movies," *Journal of Intelligent and Fuzzy Systems*, vol. 32, no. 5, pp. 3297–3311, 2017.
- [14] T. Alexopoulou, M. Michel, A. Murakami, and D. Meurers, "Task effects on linguistic complexity and accuracy: a large-scale learner corpus analysis employing natural language processing techniques," *Language Learning*, vol. 67, no. S1, pp. 180–208, 2017.
- [15] S. De Jans, D. Van de Sompel, L. Hudders, and V. Cauberghe, "Advertising targeting young children: an overview of 10

- years of research (2006-2016),” *International Journal of Advertising*, vol. 38, no. 2, pp. 173–206, 2019.
- [16] F. M. Schneider, “Measuring subjective movie evaluation criteria: conceptual foundation, construction, and validation of the SMEC scales,” *Communication Methods and Measures*, vol. 11, no. 1, pp. 49–75, 2017.
- [17] M. A. Mizher, A. A. Mazhar, M. C. Ang, and M. A. Mizher, “A review of video falsifying techniques and video forgery detection techniques,” *International Journal of Electronic Security and Digital Forensics*, vol. 9, no. 3, pp. 191–208, 2017.
- [18] J. T. Fisher, J. R. Keene, R. Huskey, and R. Weber, “The limited capacity model of motivated mediated message processing: taking stock of the past,” *Annals of the International Communication Association*, vol. 42, no. 4, pp. 270–290, 2018.
- [19] V. Grech, “The application of the mayer multimedia learning theory to medical powerpoint slide show presentations,” *Journal of Visual Communication in Medicine*, vol. 41, no. 1, pp. 36–41, 2018.
- [20] J. Black, M. Barzy, D. Williams, and H. Ferguson, “Intact counterfactual emotion processing in autism spectrum disorder: evidence from eye-tracking,” *Autism Research*, vol. 12, no. 3, pp. 422–444, 2019.
- [21] P. Tashman, V. Marano, and J. Babin, “Firm-specific assets and the internationalization-performance relationship in the U.S. movie studio industry,” *International Business Review*, vol. 28, no. 4, pp. 785–795, 2019.